Long-wave anisotropy in stratified media:
A numerical test

J. M. Carcione*, D. Kosloff‡, and A. Behle§

ABSTRACT

When a seismic signal propagates in a stratified earth, there is anisotropy if the dominant wavelength is long enough compared to the layer thickness. In this situation, the layered medium can be replaced by an equivalent nondispersive transversely isotropic medium. Theoretical and experimental analyses of the required minimum ratio of seismic wavelength to layer spacing based on kinematic considerations yield different results, with a much higher value in the experimental test.

The present work investigates the effects of layering by wave simulation and attempts to establish quantitatively the minimum ratio for which the long-wave approximation starts to be valid. We consider two-constituent periodically layered media and analyze the long-wave approximation for different material compositions and different material proportions in 1-D and 2-D media. The evaluation of the minimum ratio compares snapshots and synthetic seismograms visually and through a measure of coherence.

Layering induces scattering with wave dispersion or anisotropy depending upon the wavelength-to-layer thickness ratio. The modeling confirms the dispersive characteristics of the wave field, the scattering effects in the form of coda waves at short wavelengths, and the smoothed transversely isotropic behavior at long wavelengths. 1-D numerical tests for different media indicate that the minimum ratio is highest for the midrange of compositions, i.e., equal amount of each material, and for stronger reflection coefficients between the constituents. For epoxy-glass, the value is around $R = 8$, while for sandstone-limestone, it is between $R = 5$ and $R = 6$. Recent wave-propagation experiments done in epoxy-glass also imply a highest minimum ratio for midrange of composition; however, the 1-D numerical tests confirm the long-wave approximation at shorter wavelengths than experimentally. The 2-D case shows that the more anisotropic the equivalent medium, the higher the minimum ratio, and that the approximation depends upon the propagation angle with longer wavelengths required in the direction of the layering.

INTRODUCTION

In the earth, although many of the materials are intrinsically anisotropic (for instance, many of the metamorphic and igneous rocks), their random orientation gives rise to a material which behaves isotropically when the dominant wavelength of the wave field is long compared to the crystal dimensions. However, due to the layered nature of sedimentary formations, transverse isotropy occurs when the dominant wavelength is long enough compared with the dimen-sions of the layers (Riznichenko, 1949; Postma, 1955; Krey and Helbig, 1956; Rytov, 1956; Backus, 1962). Wave propagation effects in stratified media depend on the wavelength of the signal. For wavelengths short compared to the dimensions of the layers, scattering in the form of coda waves is present. Thus, these wavelengths show dispersive behavior, i.e., the velocity is frequency dependent. On the other hand, at long wavelengths or low frequencies, the medium behaves as a nondispersive, smoothed, transversely isotropic material.

Helbig (1984) analyzed the dispersion relation for *SH*-waves in a periodic layered medium and in the long-wave equivalent transversely isotropic medium. He showed that the equivalence is valid for wavelengths larger than three times the spatial period of layering. Melia and Carlson (1984) made experimental laboratory measurements of compressional wave velocities parallel and perpendicular to a periodic stratified medium consisting of glass and epoxy layers. They concluded that the long-wave approximation holds when the ratio *R* lies between 10 and 100, and that the minimum ratio is highest in the midrange of compositions, i.e., half glass and half epoxy.

Recently, numerical modeling has begun to be used as a tool for investigating the effects of layering on wave propagation (Carcione, 1987; Egan, 1989; Esmersoy et al., 1989; Kerner, 1989; and Philippe and Bouchon, 1989). The present work is an attempt to establish quantitatively the minimum value of the ratio $R = \lambda_0/d$ for which a periodic layered medium can be replaced by a homogeneous transversely isotropic medium, where λ_0 is the dominant wavelength of the signal, and is the spatial period of the stratified system. We restrict our analysis to a two-constituent, spatially periodic medium. We refer to the periodic, isotropic, two-layered system as the PL medium, and the transversely isotropic, long-wave equivalent medium as the TIE medium.

The analysis is performed by simulating wave propagation through an epoxy-glass sequence, as in Melia and Carlson's experiment, and a limestone-sandstone sequence, as used by Postma to demonstrate the anisotropic properties of layering. These systems are representative of many solids in material science and of layered formations in the earth, and have different degrees of anisotropy and impedance constrasts. The simulations are carried out by solving the wave equation numerically for both the PL and the TIE media in 1-D and 2-D models. Since the wave-propagation process is linear, synthetic seismograms for different dominant wavelengths λ_0 are obtained with a single simulation by considering a space-time spike as force and then performing the time convolution with the source time function.

We establish the minimum ratio *R* by comparing the wave fields through a measure of coherence. The evaluation is made for different material proportions and for different values of the source's dominant frequency (or different *R* values) for a given spatial period. Visual comparisons between snapshots and between synthetic seismograms also establish the ratio qualitatively. The proposed numerical experiments account for not only the kinematics but also the amplitude of the wave field. This evaluation can be considered conclusive, since the analysis with theoretical solutions is restricted by the complexity of the problem, and laboratory measurements are never exact due to experimental uncertainty.

The paper's main sections analyze the problem in 1-D and 2-D media, respectively. We first establish the constitutive relations, then the equations of motion; finally, we present the results of the numerical experiments. The numerical algorithm is tested with an analytical solution in order to be sure that effects such as scattering and dispersion are well described by the modeling scheme.

ONE-DIMENSIONAL MEDIA

The layered medium

The one-dimensional (1-D) stress-strain relation for each material component is given by

$$\sigma = M \frac{\partial u}{\partial x}, \tag{1}$$

where $\sigma(x, t)$ and $u(x, t)$ are the stress and displacement wave fields, respectively, depending upon the position x and the time variable t. $M(x)$ is the elastic modulus.

Assuming that each material contributes with a relative proportion P_i, we have $\Sigma P_i = 1$, where the summation is over the number of different materials. For the particular case considered in this work, i.e., a PL medium with two constituents, the relative proportions are given by

$$P_1 = \frac{d_1}{d},$$

and   (2)

$$P_2 = \frac{d_2}{d},$$

where d_1 and d_2 are the corresponding layer thicknesses, with spatial period

$$d = d_1 + d_2. \tag{3}$$

The equivalent medium

When the dominant wavelength of the signal is long enough compared to the spatial period, the PL medium can be replaced by a TIE medium. In the 1-D case the constitutive relation of this medium is

$$\sigma = \overline{M} \frac{\partial u}{\partial x}, \tag{4}$$

where the averaged elastic modulus is given by

$$\overline{M} = \langle M^{-1} \rangle^{-1}. \tag{5}$$

The averaging process is performed by the bracket operation, which for sequences consisting of two distinct materials is

$$\langle A \rangle = A_1 P_1 + A_2 P_2 \tag{6}$$

for a given physical quantity A.

Equation (5) is the expression for the averaged $\bar{c}_{33}$ in the symmetry axis of a transversely isotropic solid (see Postma, 1955), since the 1-D problem is equivalent to the problem of considering plane waves propagating in the symmetry axis direction. Using equations (2), (3), and (6), the average modulus (5) is given by

$$\overline{M} = \frac{M_1 M_2 (d_1 + d_2)}{d_1 M_2 + d_2 M_1}. \tag{7}$$

Similarly, the average density is

$$\bar{\rho} = \langle \rho \rangle = \frac{\rho_1 d_1 + \rho_2 d_2}{d_1 + d_2}, \tag{8}$$

with ρ_1 and ρ_2 the densities of the individual layers.

The equation of motion

The 1-D wave equation for the displacement field is

$$\frac{1}{\gamma}\frac{\partial}{\partial x}E\frac{\partial u}{\partial x} = \ddot{u} + \frac{f}{\gamma}, \tag{9}$$

where $E = M(x)$, $\gamma = \rho(x)$ in the PL medium, and $E = \overline{M}(x)$, $\gamma = \bar{\rho}(x)$ in the TIE medium. $f(x, t)$ is the body force and a dot above a variable denotes time differentiation. The body force is taken as

$$f(x, t) = \delta(x - x_0)\delta(t), \tag{10}$$

where $\delta(x - x_0)$ means a discrete delta located at $x = x_0$ and $\delta(t)$ a time delta function indicating that the motion begins at $t = 0$.

The dominant wavelength of the signal is defined in the long-wave approximation by

$$\lambda_0 = \frac{\overline{V}}{f_0}, \tag{11}$$

where

$$\overline{V} = \left(\frac{\overline{M}}{\bar{\rho}}\right)^{1/2} \tag{12}$$

is the average velocity, and f_0 is the source's dominant frequency. We define R as the ratio of dominant wavelength λ_0 to spatial period d:

$$R = \frac{\lambda_0}{d}. \tag{13}$$

The aim of this work is to find the minimum R for which the long-wave approximation starts to be valid.

Equation (9) is solved numerically by using the Chebychev spectral method as a time integration and the Fourier method to compute the spatial derivatives. A detailed description of the algorithm can be found in Carcione et al. (1988). After the synthetic seismograms are obtained with the body force given in equation (10), they are convolved with a causal zero-phase time function given by

$$h(t) = e^{2f_0^2(t - t_0)^2}\cos[2\pi f_0(t - t_0)], \tag{14}$$

where t_0 is a constant time delay. The amplitude spectrum of $h(t)$ is represented in Figure 1, where the cutoff frequency is $2f_0$. This method for computing the system response to a band-limited function is valid since the wave propagation process is linear. In this way it is possible to compute synthetic seismograms for different dominant frequencies with minimum cost in computing time.

1-D numerical tests

The properties of the isotropic materials are given in Table 1 with the respective P-wave and S-wave impedances. The average modulus is calculated by using equation (7), considering that $M = V_p^2\rho$ for the individual layers. The average velocities, given by equation (12), are listed in Table 2 for different material proportions, together with the average densities. Discretization of the space implies that $d_1 = n_1 DX$ and $d_2 = n_2 DX$, with DX the grid spacing and n_1 and n_2
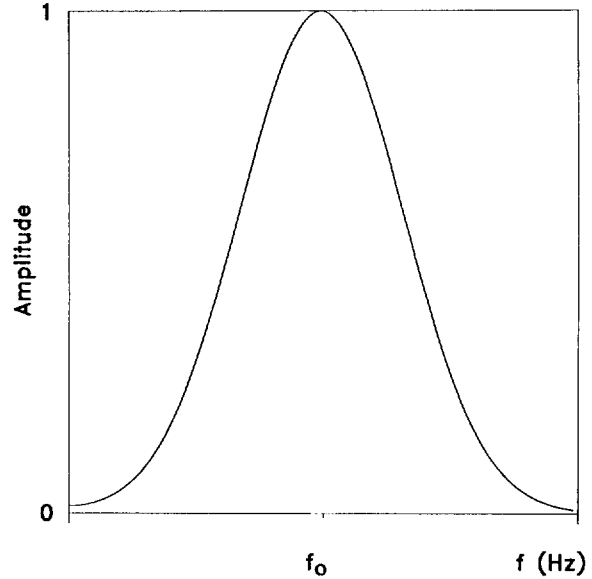

FIG. 1. Amplitude spectrum of the source given in equation (14). f_0 is the dominant frequency.

Table 1. Material properties of the PL media.

Material	V_P (m/s)	V_S (m/s)	ρ (Kg/m^3)	Z_P (Kg/s/ m^2 × 10^3)	$(Z_s$ (Kg/s m^2 × 10^3)
Epoxy	2530	1200	1120	2833	1344
Glass	5560	3200	2510	13955	8032
	2530	1200	1815	4591	2178
	5560	3200	1815	10091	5808
Sandstone	2950	1620	2300	6785	3726
Limestone	5440	3040	2700	14688	8208

Table 2. Material properties of the 1-D TIE media.

	P_2	n_1	n_2	$\overline{V}$ (m/s)	$\bar{\rho}$ (Kg/m^3)
Epoxy-glass	0.25	3	1	2513	1467
	0.50	2	2	2689	1815
ρ (const)	0.50	2	2	3256	1815
	0.75	1	3	3222	2162
Sandstone-limestone	0.50	2	2	3578	2500

natural numbers. Thus, the spatial period is $d = (n_1 + n_2)DX$ and, from equation (2),

$$n_1 = (1 - P_2) \frac{d}{DX},$$

$$n_2 = P_2 \frac{d}{DX}.$$

(15)

By choosing, for instance, $d/DX = 4$, we obtain the different relative proportions in Table 2. In the following examples the subindex nomenclature is $(1, 2) \equiv (e, g)$ for the epoxy-glass periodic solid, and $(1, 2) \equiv (\ell, s)$ for the limestone-sandstone periodic medium. The number of grid points is $NX = 385$, with $DX = 0.25$ mm grid spacing for epoxy-glass and $DX = 25$ m for sandstone-limestone; therefore, the spatial periods are $d = 1$ mm and $d = 100$ m, respectively.

First, we test the numerical algorithm in the problem of wave propagation through a PL medium with $P_g = 0.50$. The analytical solution is calculated with a propagator matrix

method (Haskell, 1953). Figure 2 compares numerical and analytical solutions for the particle velocity $(\dot{u})$ for two different values of the source dominant frequency, (a) $f_0 = 0.3$ MHz, and (b) $f_0 = 0.6$ MHz. The agreement is very good, which assures that dispersion and scattering are correctly described with the modeling.

Snapshots and synthetic seismograms between the PL and the TIE media are compared by using the semblance

$$S(\%) = 100 \frac{\sum (a_i + b_i)^2}{2 \sum (a_i^2 + b_i^2)},$$

(16)

for a given discrete series a and b where the summation is over the number of samples.
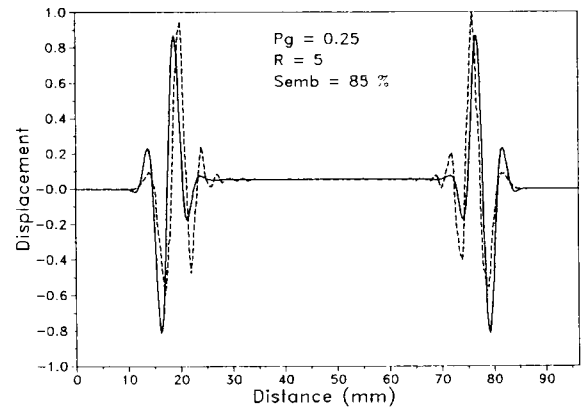
Figure 3 represents snapshots of the displacement field at $t = 15$ μs with the source located at grid point 192, for $R = 5$, and two different material proportions, (a) $P_g = 0.25$ and (b) $P_g = 0.50$. The dashed line is for the PL medium and the continuous line for the TIE medium. The best agreement is when $P_g = 0.25$. These results confirm that the long-wave
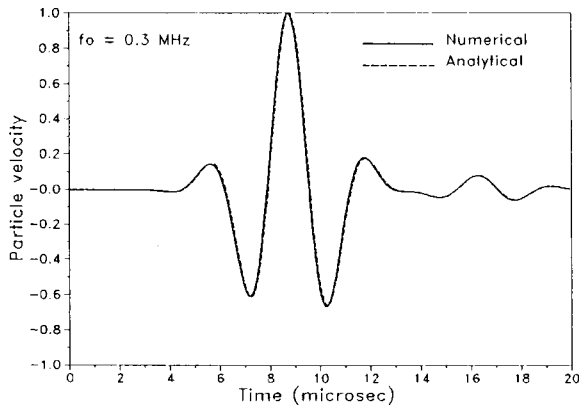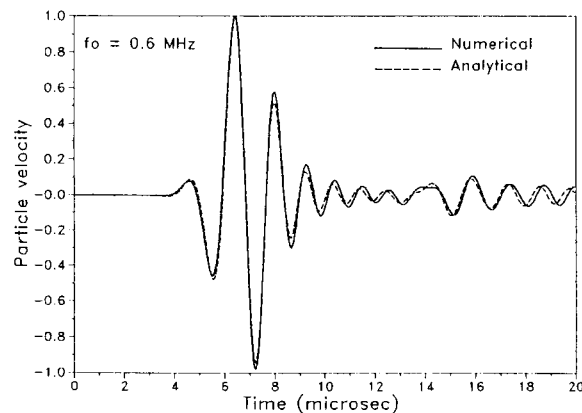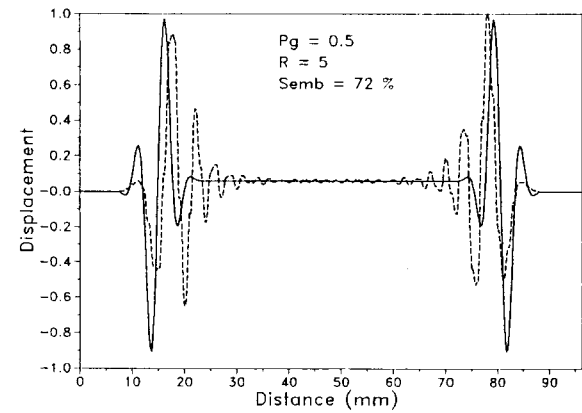

(a)



(b)

FIG. 2. Comparison between numerical and analytical solutions in a 1-D PL epoxy-glass medium with $P_g = 0.50$, where (a) $f_0 = 0.3$ MHz and (b) $f_0 = 0.6$ MHz.

(a)

(b)

FIG. 3. 1-D snapshot comparison at $t = 15$ μs in epoxy-glass for $R = 5$ and two different material proportions, where (a) $P_g = 0.25$ ($d_e = 0.75$ mm and $d_g = 0.25$ mm) and $P_g = 0.50$ ($d_e = d_g = 0.5$ mm). The dashed and continuous lines correspond to the PL and TIE media, respectively.

approximation is a function of the proportions of the materials as found experimentally by Melia and Carlson (1984). They concluded that the minimum ratio was highest in the midrange of compositions ($P_g = 0.50$).

Figure 4 displays synthetic seismograms of the displacement field in a receiver located at gridpoint 142, for $P_g = 0.50$, where (a) $R = 3$, (b) $R = 5$, and (c) $R = 8$. The continuous line corresponds to the TIE media. The results
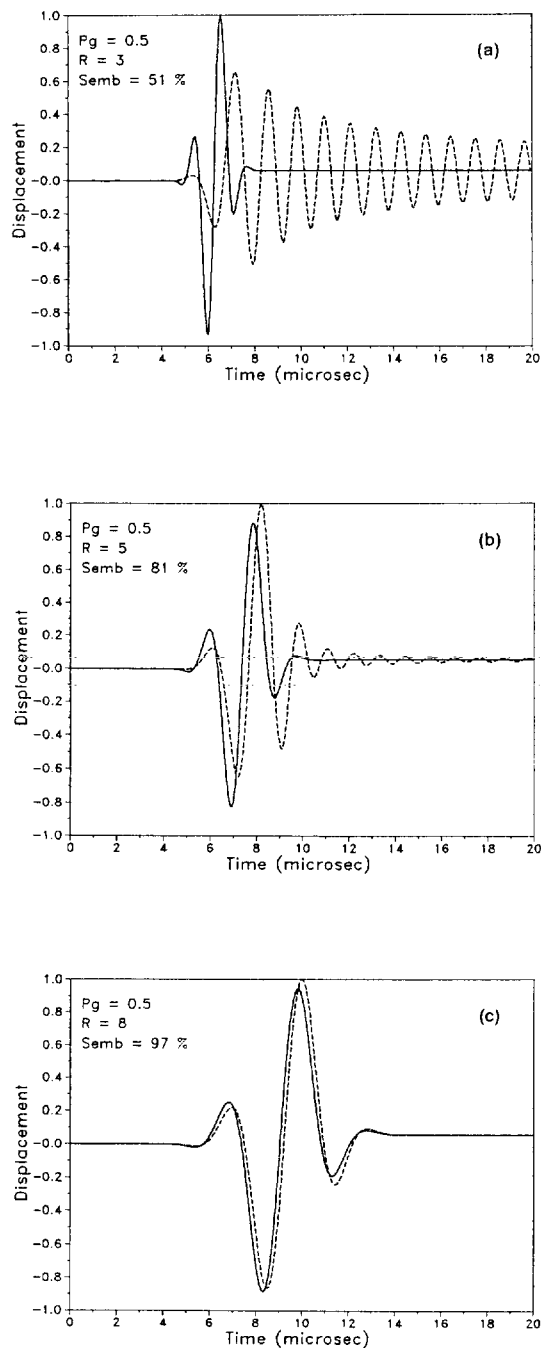
for the semblance are summarized in Table 3, where the cases $P_g = 0.25$ and $P_g = 0.75$ are also included. As in the previous example, $P_g = 0.50$ gives the lowest values for the semblance. When $R = 3$, i.e., the dominant wavelength is three times the spatial period, the PL medium induces scattering which causes the coda waves, strongest for $P_g = 0.50$. Moreover, for different values of R, the peak of the primary pulse has different arrival times. This means that the medium is dispersive, i.e., the velocity varies with wavelength. For this system, the long-wave approximation seems to be valid when $R > 8$ if we consider that a value greater than 97 percent for the semblance makes the PL and TIE media equivalent. As such, for wavelengths greater than eight times the spatial period, the medium behaves nondispersively. For illustration, Figure 5 represents the variation of the semblance with R for the case $P_g = 0.50$. As can be seen, the curve becomes flat at $R = 8$.

To study the influence of the density, we consider a PL epoxy-glass system with $\rho_e = \rho_g = 1815$ Kg/m^3 which is the average density when $P_g = 0.50$. The average velocity for this system when $P_g = 0.50$ is given in Table 2. The values of the semblance for $R = 3, 5$, and 8 are $S = 65, 95$, and 99 percent, respectively. These results indicate that the minimum ratio is between $R = 5$ and $R = 6$, although it is not clear that this is because the density is constant. The next example helps clarify this point.

Fig. 4. Synthetic seismogram comparisons in 1-D epoxy-glass for $P_g = 0.50$ ($d_e = d_g = 0.5$ mm), where (a) $R = 3$, (b) $R = 5$, and (c) $R = 8$. The dashed and continuous lines correspond to the PL and TIE media, respectively.

Table 3. Semblance (%) (epoxy-glass system).

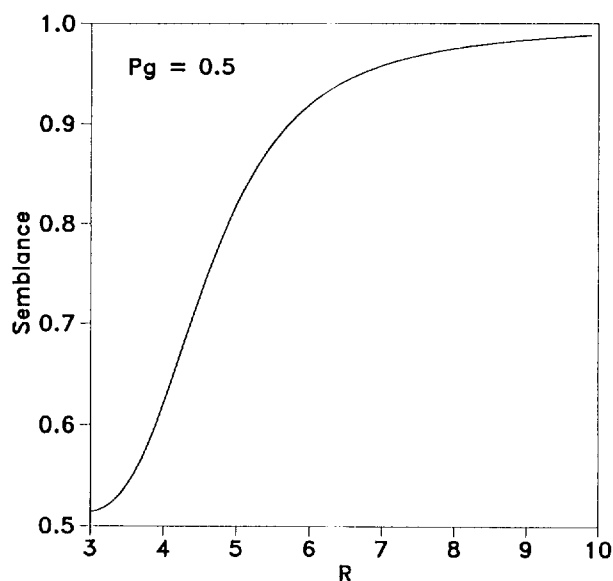|		R		
		3	5	8
	0.25	56	91	98
P_g	0.50	51	81	97
	0.75	56	83	98

Fig. 5. Semblance versus ratio of dominant wavelength spatial period for $P_g = 0.50$ in epoxy-glass.

Let us consider a PL medium composed of sandstone and limestone whose properties are given in Table 1. The average velocity and density of the TIE medium for $P_\ell = 0.50$ are given in Table 2. The system is composed of alternating layers, each 50 m thick. Figure 6 displays synthetic seismograms for (a) $R = 3$, (b) $R = 5$, and (c) $R = 8$. The values of the semblance are similar to those obtained for constant density with the epoxy-glass system. Again, the long-wave approximation seems to be valid between $R = 5$ and $R = 6$. This difference to the variable-density epoxy-glass system, for which the minimum ratio is around $R = 8$, suggests that the long-wave approximation depends upon the impedance contrast between the constituents, i.e., on the reflection coefficients. Thus, weaker reflectivity implies that the long-wavelength approximation takes place for smaller values of R. From Table 1, $\Delta Z_p = 11\ 122\ 10^3$ Kg/s/m^2 and $\Delta Z_p = 5500$

10^3 Kg/s/m^2 for the variable and constant-density epoxy-glass systems, respectively, and $\Delta Z_p = 7900 \times 10^3$ Kg/s/m^2 for the sandstone-limestone system. They give reflection coefficients of $R_p = 0.66$ (epoxy-glass), $R_p = 0.37$ (constant-density epoxy-glass), and $R_p = 0.37$ (sandstone-limestone). These facts explain why the results between the constant-density epoxy-glass system and the sandstone-limestone sequence are identical.

TWO-DIMENSIONAL MEDIA

The layered medium

The constitutive relation of each individual component of the 2-D layered medium can be expressed in matrix notation as

$$\begin{bmatrix} \sigma_{xx} \\ \sigma_{zz} \\ \sigma_{xz} \end{bmatrix} = \begin{bmatrix} \lambda + 2\mu & \lambda & 0 \\ \lambda & \lambda + 2\mu & 0 \\ 0 & 0 & \mu \end{bmatrix} \begin{bmatrix} \varepsilon_{xx} \\ \varepsilon_{zz} \\ 2\varepsilon_{xz} \end{bmatrix}, \quad (17)$$

where the σ's and the ε's are stress and strain components, respectively, depending upon the position vector $\mathbf{r} = (x, z)$ and the time variable t. $\lambda(\mathbf{r})$ and $\mu(\mathbf{r})$ are the Lamé constants.

As in the 1-D case, we assume that the material is a two-constituent, spatially periodic medium with relative proportions and spatial period given by equations (2) and (3). Lamination is taken parallel to the x-axis, i.e., z is parallel to the symmetry axis.

The equivalent medium

In the long-wave approximation the layered medium is equivalent to a homogeneous transversely isotropic medium with stress-strain relation given by

$$\begin{bmatrix} \sigma_{xx} \\ \sigma_{zz} \\ \sigma_{xz} \end{bmatrix} = \begin{bmatrix} \bar{c}_{11} & \bar{c}_{13} & 0 \\ \bar{c}_{13} & \bar{c}_{33} & 0 \\ 0 & 0 & \bar{c}_{55} \end{bmatrix} \begin{bmatrix} \varepsilon_{xx} \\ \varepsilon_{zz} \\ 2\varepsilon_{xz} \end{bmatrix}, \quad (18)$$

where the averaged elasticities are calculated as (Backus, 1962)

$$\bar{c}_{11} = \langle 4\mu(\lambda + \mu)(\lambda + 2\mu)^{-1} \rangle$$
$$+ \langle (\lambda + 2\mu)^{-1} \rangle^{-1} \langle \lambda(\lambda + 2\mu)^{-1} \rangle^2, \quad (19a)$$

$$\bar{c}_{13} = \langle (\lambda + 2\mu)^{-1} \rangle^{-1} \langle \lambda(\lambda + 2\mu)^{-1} \rangle, \quad (19b)$$

$$\bar{c}_{33} = \langle (\lambda + 2\mu)^{-1} \rangle^{-1}, \quad (19c)$$

and

$$\bar{c}_{55} = \langle \mu^{-1} \rangle^{-1}. \quad (19d)$$

In the case of a periodic sequence composed of two alternating plane, parallel, and homogeneous isotropic layers, equations (19) lead to the averaged elasticities obtained by Postma (1955). The average density is given by equation (8).

The equation of motion

The equation of motion for a 2-D transversely isotropic medium can be expressed as (Carcione et al., 1988)

$$\gamma \ddot{u}_x = \frac{\partial}{\partial x}\left[c_{11}\frac{\partial u_x}{\partial x} + c_{13}\frac{\partial u_z}{\partial z}\right]$$
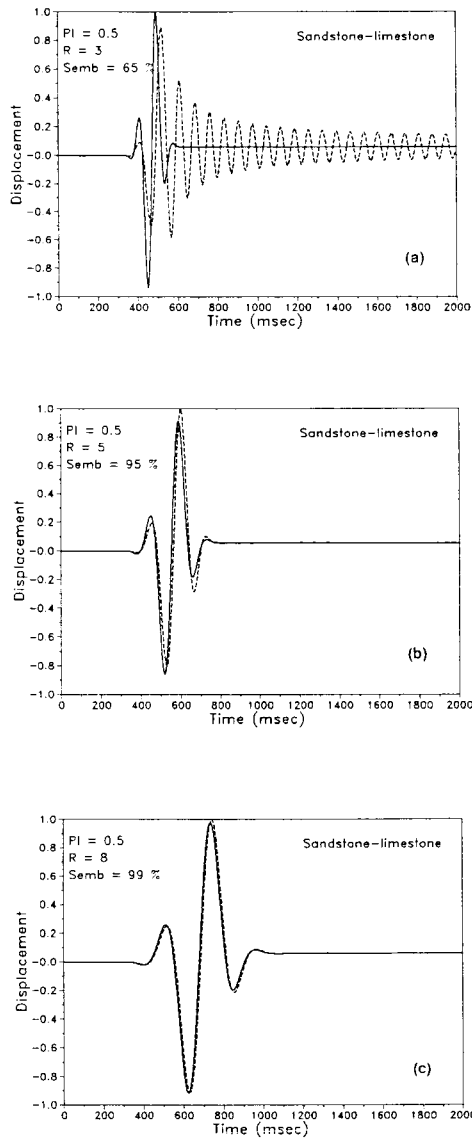

FIG. 6. Synthetic seismogram comparisons in 1-D sandstone-limestone for $P_\ell = 0.50$ ($d_s = d_\ell = 50$ m), where (a) $R = 3$, (b) $R = 5$, and (c) $R = 8$. The dashed and continuous lines correspond to the PL and TIE media, respectively.

$$+ \frac{\partial}{\partial z} \left[c_{55} \left(\frac{\partial u_x}{\partial z} + \frac{\partial u_z}{\partial x} \right) \right] + f_x, \qquad (20a)$$

$$\gamma \ddot{u}_z = \frac{\partial}{\partial z} \left[c_{13} \frac{\partial u_x}{\partial x} + c_{33} \frac{\partial u_z}{\partial z} \right]$$

$$+ \frac{\partial}{\partial x} \left[c_{55} \left(\frac{\partial u_x}{\partial z} + \frac{\partial u_z}{\partial x} \right) \right] + f_z, \qquad (20b)$$

where u_x and u_z are the horizontal and vertical displacements and f_x and f_z are the source components.

For the homogeneous TIE medium, $c_{11} = \bar{c}_{11}$, $c_{13} = \bar{c}_{13}$, $c_{33} = \bar{c}_{33}$, $c_{55} = \bar{c}_{55}$, and $\gamma = \bar{\rho}$; and for the layered medium, $c_{11} = c_{33} = \lambda + 2\mu$, $c_{13} = \lambda$, $c_{55} = \mu$, and $\gamma = \rho$. The source components are

$$f_x(\mathbf{r}, t) = 0$$

and   (21)

$$f_z(\mathbf{r}, t) = \delta(\mathbf{r} - \mathbf{r}_0)\delta(t).$$

As in the 1-D case, $\delta(\mathbf{r} - \mathbf{r}_0)$ means a discrete delta located at $\mathbf{r}_0 = (x_0, z_0)$. The compressional and shear dominant wavelengths are given by

$$\lambda_0^{(P)} = \frac{\bar{V}_P}{f_0},$$

and   (22)

$$\lambda_0^{(S)} = \frac{\bar{V}_S}{f_0},$$

FIG. 8. Snapshots at 27 μs in 2-D epoxy-glass for a dominant frequency for the source of $f_0 = 0.2$ MHz, where (a) are the PL media and (b) the TIE media. Thicknesses are $d_e = d_g = 0.5$ mm. The dominant wavelengths along the symmetry axis direction are $\lambda^{(P)} = 13.44$ mm and $\lambda^{(S)} = 6.46$ mm.
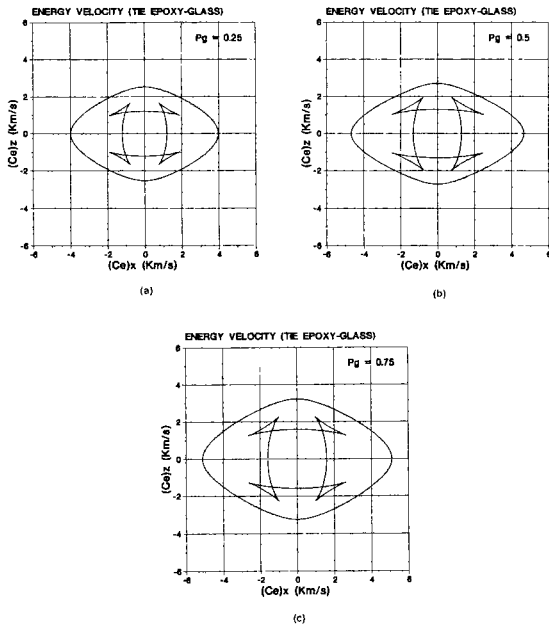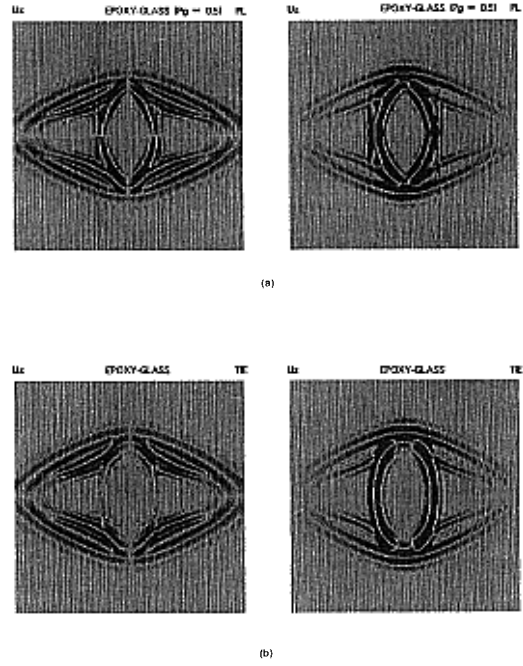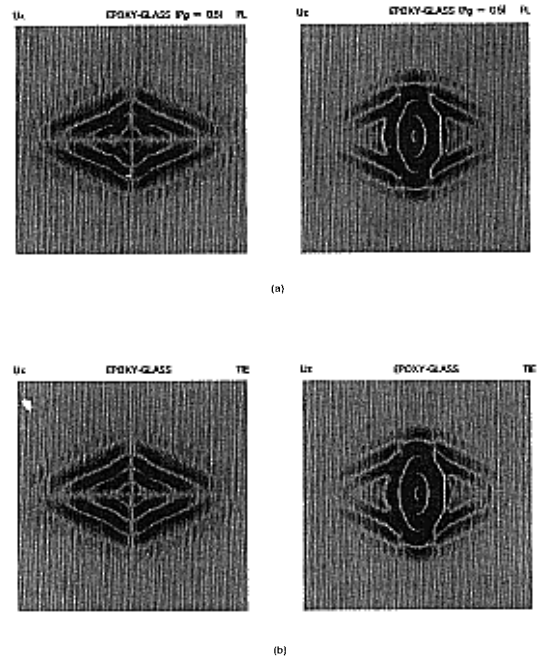

FIG. 7. Energy velocity curves for epoxy-glass of different material proportions: (a) $P_g = 0.25$, (b) $P_g = 0.50$, and (c) $P_g = 0.75$. The outer and inner curves correspond to the quasi-P and quasi-S waves, respectively.

FIG. 9. Snapshots at 27 μs in 2-D epoxy-glass for a dominant frequency for the source of $f_0 = 0.1$ MHz, where (a) are the PL media and (b) the TIE media. Thicknesses are $d_e = d_g = 0.5$ mm. The dominant wavelengths along the symmetry axis direction are $\lambda^{(P)} = 26.88$ mm and $\lambda^{(S)} = 12.92$ mm.

Table 4. Material properties of the 2-D TIE media.

	P_2	n_1	n_2	$\bar{c}_{11}$ (GPa)	$\bar{c}_{13}$ (GPa)	$\bar{c}_{33}$ (GPa)	$\bar{c}_{55}$ (GPa)	$\bar{\rho}$ (Kg/m^3)	A (%)
Epoxy-glass	0.25	3	1	23.2	4.6	9.7	2.1	1467	22.5
	0.50	2	2	39.4	5.8	13.1	3.0	1815	26.8
	0.75	1	3	56.2	8.7	22.4	5.4	2162	22.5
Sandstone-limestone	0.50	1	1	47.5	12.3	32.0	9.7	2500	9.8

where $\bar{V}_p$ and $\bar{V}_s$ are the P and S energy velocities of the TIE medium. Note that these velocities depend upon the propagation direction as do the dominant wavelengths. As before, we define the ratios

$$R^{(P)} = \frac{\lambda_0^{(P)}}{d},$$

$$R^{(S)} = \frac{\lambda_0^{(S)}}{d}.$$

(23)

Equations (20) are solved numerically by using the Cheby-chev spectral method (Carcione et al., 1988). Synthetic seismograms are calculated as in the 1-D problem with the source time function given by equation (14).

Material properties and wave characteristics

The 2-D stratified medium is composed of alternating plane layers with thicknesses d_1 and d_2. The material properties are given in Table 1. Considering that $\lambda = (V_P^2 - 2V_S^2)\rho$ and $\mu = V_S^2\rho$, and using equations (19), we get the elasticities and density of the TIE medium for the different relative proportions given by equation (2), and spatial period

given by equation (3). The material properties of the long-wavelength transversely isotropic media are illustrated in Table 4, where

$$A(\%) = 100 \, \frac{V_P(\theta = \pi/2) - V_P(\theta = 0)}{V_P(\theta = \pi/2) + V_P(\theta = 0)}$$

$$= 100 \, \frac{\bar{c}_{11}^{1/2} - \bar{c}_{33}^{1/2}}{\bar{c}_{11}^{1/2} + \bar{c}_{33}^{1/2}}$$

(24)

is the quasi-P wave anisotropy, with V_P the quasi-P wave energy velocity, and θ the angle between the symmetry axis and the propagation direction. The highest degree of anisotropy is around $P_g = 0.50$. The energy velocity curves (equivalent to the wavefront curves) are illustrated in Figure 7 for different glass proportions: (a) $P_g = 0.25$, (b) $P_g = 0.50$, and (c) $P_g = 0.75$. The outer and inner curves correspond to the quasi-P and quasi-S waves, respectively. Expressions for the energy velocities can be found in Carcione et al. (1988).
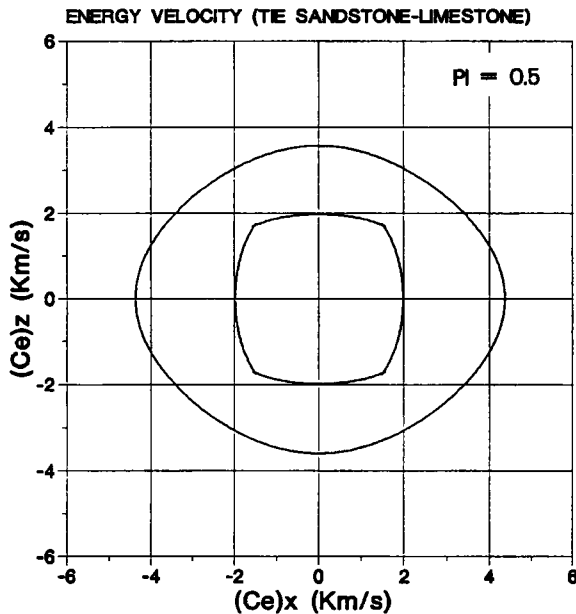
FIG. 10. Energy velocity curves in sandstone-limestone for $P_\ell = 0.50$. The outer and inner curves correspond to the quasi-P and quasi-S waves, respectively.
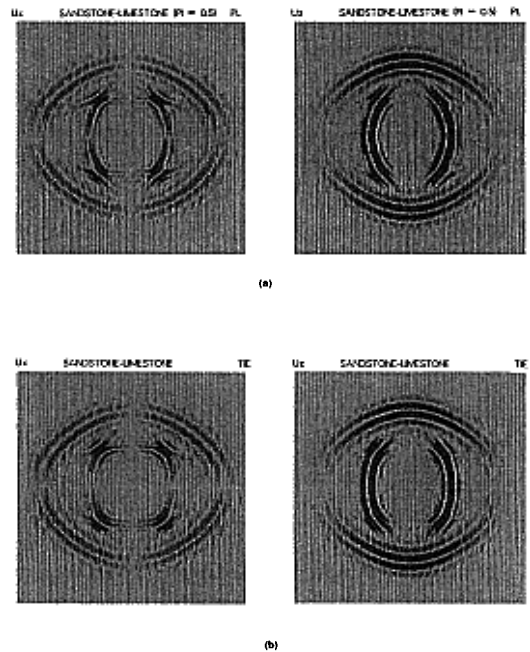
FIG. 11. Snapshots at 0.48s in sandstone-limestone for a dominant frequency for the source of $f_0 = 12$ Hz, where (a) are the PL media and (b) the TIE media. Thicknesses are $d_s = d_\ell = 10$ m. The dominant wavelengths along the symmetry axis direction are $\lambda^{(P)} = 349$ m and $\lambda^{(S)} = 157$ m.
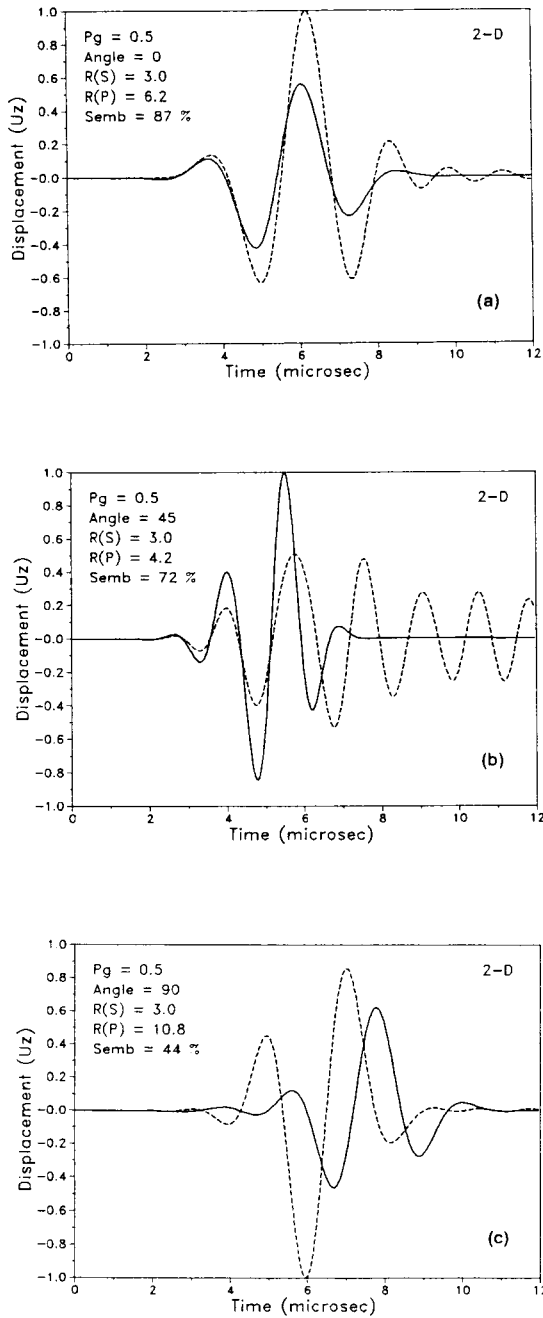
FIG. 12. Synthetic seismogram comparisons in 2-D epoxy-glass for $P_g = 0.50$ ($d_e = d_g = 0.50$ mm), where (a) $\theta = 0$, (b) $\theta = 45$, and (c) $\theta = 90$ degrees, and the receivers are located 5 mm from the source. The dashed and continuous lines correspond to the PL and TIE media, respectively.

Table 5. Semblance (%) (2-D glass-epoxy system).

	Angle (degrees)		
	0	45	90
0.25	90	57	99
P_g 0.50	87	72	44
0.75	95	83	31

The TIE medium is class V according to the classification given by Payton (1983, p. 26) for which the phase velocity curve presents four bitangents and the wavefront curve, four cuspidal triangles at $\theta = 45$ degrees, as seen in Figure 7. This classification depends upon the particular value of the elasticities which are constrained by certain inequalities. A theoretical evaluation of these constraints for the TIE medium appears quite cumbersome, although numerical verifications for different layered media indicate that the equivalent medium is always class V.

2-D numerical tests

We consider PL media with interfaces parallel to the X-axis. All the examples in this section use $NX = NZ = 405$ and a vertical source located at gridpoints (202, 202). First we compute snapshots in an epoxy-glass system with $P_g = 0.50$ and spatial period $d = 1$ mm. Grid spacing is $DX = DZ = 0.5$ mm. The results are displayed in Figures 8 and 9, for source dominant frequencies of $f_0 = 0.2$ MHz and $f_0 = 0.1$ MHz, respectively, where (a) is the PL medium and (b) is the TIE medium. The propagating time is 27 μs. The values of the ratios, as given by equation (23), depend upon the angle θ between the symmetry axis and the propagation direction. For $f_0 = 0.2$ MHz, they are $R^{(P)}(\theta = 0$ degrees$) = 13.44$, $R^{(P)}(\theta = 90$ degrees$) = 23.31$, and $R^{(S)}(\theta = 0$ degrees$) = R^{(S)}(\theta = 90$ degrees$) = 6.46$. For $f_0 = 0.1$ MHz, these values should be multiplied by a factor of two. When $f_0 = 0.2$ MHz, as in Figure 8, the P-wave shows no differences between the PL and the TIE media, but the S-wave has important differences around $\theta = 90$ degrees, while the cusps are perfectly equivalent. These differences are more pronounced in the u_x component. Figure 9 shows that, when $f_0 = 0.1$ MHz, the two media are completely equivalent.

As mentioned, the case $P_g = 0.50$ shows the highest degree of quasi-P-wave anisotropy with $A = 26.8$ percent. The 2-D sandstone-limestone TIE medium is less anisotropic, with a value of $A = 9.8$ percent for $P_\ell = 0.50$ as indicated in Table 4. The energy velocity curves for this material are represented in Figure 10. Comparing these curves with those of Figure 7b, it can be seen that the quasi-S wave is also more anisotropic in the epoxy-glass system.

To compare results between the two systems, we compute snapshots in PL and TIE sandstone-limestone media. For $P_\ell = 0.50$, we take $DX = DZ = d_s = d_\ell = 10$ m, i.e., a spatial period $d = 20$ m, and a dominant frequency for the source of $f_0 = 12$ Hz. Snapshots at 0.48 s are shown in Figure 11, where (a) is the PL medium and (b) the TIE medium. The ratios are $R^{(P)}(\theta = 0$ degrees$) = 17.44$, $R^{(P)}(\theta = 90$ degrees$) = 14.31$, and $R^{(S)}(\theta = 0$ degrees$) = R^{(S)}(\theta = 90$ degrees$) = 7.88$, which are comparable with the values for the epoxy-glass test at $f_0 = 0.2$ MHz. From Figure 8 it is clear that the long-wavelength approximation is not valid for the S-wave (inner wavefront), while it applies to the sandstone-limestone system as seen from Figure 11. Thus, the more anisotropic the TIE medium, the higher the minimum ratio.

Finally, we computed synthetic seismograms in PL media with different material proportions. These simulations use $DX = DZ = 0.25$ mm, with spatial periods $d = 1$ mm and

thicknesses as in the 1-D problem but in the z-direction. The seismograms for $P_g = 0.50$ are represented in Figure 12, where (a) $\theta = 0$ degrees, (b) $\theta = 45$ degrees, and (c) $\theta = 90$ degrees. The receivers are located 500 m from the source.

To compare seismograms with dissimilar material proportions, we chose the source's dominant frequency for different angles such that the ratio for S-waves has a common value $R^{(S)} = 3$. The values of $R^{(P)}$ for $P_g = 0.5$ are indicated in Figure 12, while for $P_g = 0.25$ they are $R^{(P)} = 6.3, 4.9$, and 9.9, and for $P_g = 0.75$, $R^{(P)} = 6.1, 4.2$, and 9.6, corresponding to the angles $\theta = 0, 45$, and 90 degrees, respectively. The results for the semblances are summarized in Table 5. The agreement is very good at $\theta = 0$ degrees (along the symmetry axis), where only P-wave motion contributes, with $R^{(P)}$ values greater than six. As in the 1-D case, the midrange of compositions gives the lowest semblances. For $\theta = 0$ degrees, only the S-wave contributes. As mentioned, $R^{(S)} = 3$, which is not enough to apply the long-wavelength approximation. The perfect matching for $P_g = 0.25$ is due to the fact that the wave travels mainly through the epoxy layers, which have a velocity of 1200 m/s, while the TIE medium has approximately the same velocity $\overline{V}^{(S)}(\theta = 90$ degrees$) = (\bar{c}_{33}/\bar{\rho})^{1/2} = 1196$ m/s. When $P_g = 0.50$ and $P_g = 0.75$, i.e., there is more glass contribution with velocity 3200 m/s, the velocity increases in the PL medium, and the peak of the signal arrives earlier (7 and 5 μs, respectively, compared to 8 μs when $P_g = 0.25$).

Actually, it is not surprising that the long-wavelength approximation does not apply for angles far from the symmetry axis, since in these cases the wave "sees" a longer spatial period; its value approaches infinity for $\theta = 90$ degrees.

CONCLUSIONS

Using numerical modeling for simulating wave propagation in periodically layered media, we conclude that

(1) Depending upon the relation of wavelength to layer thickness, a stratified medium induces dispersion, scattering, and a smoothed transversely isotropic behavior.

(2) The minimum ratio of wavelength to layer thickness for the long-wavelength approximation to be valid is highest in the midrange of compositions, as found recently in laboratory experiments.

(3) The minimum ratio depends on material compositions through the reflection coefficients between the constituents. For instance, for epoxy-glass it is around $R = 8$, and for sandstone-limestone (which has a lower reflection coefficient) it is between $R = 5$ and $R = 6$.

(4) 2-D numerical tests reveal that the more anisotropic the equivalent medium, the higher the minimum ratio.

(5) The minimum ratio depends upon the propagation angle. For S-waves, for a given value of wavelength to spatial thickness, the long-wavelength approximation applies for angles close to the symmetry axis and even to the cusps, but not in the direction of layering.

These tests were done in periodically layered media with isotropic constituents and, in the 2-D case, by using a vertical source. Further investigations should consider nonperiodic media with anisotropic layers, as well as different source types to study the long-wavelength approximation for each wave mode in detail.

REFERENCES

Backus, G. E., 1962, Long-wave elastic anisotropy produced by horizontal layering: J. Geophys. Res., 67, 4427–4440.

Carcione, J. M., 1987, Wave propagation simulation in real media: PhD thesis, Tel-Aviv Univ.

Carcione, J. M., Kosloff, D., and Kosloff, R., 1988, Wave propagation simulation in an elastic anisotropic (transversely isotropic) solid: Quart. J. Mech. Appl. Math., 41, 319–345.

Egan, M., 1989, Dispersive and anisotropic aspects of stratigraphic filtering: Presented at the 59th Ann. Internat. Mtg., Soc. Expl. Geophys., Expanded Abstracts, 1019–1022.

Esmersoy, C., Hsu, K., and Schoenberg, M., 1989, Quantitative analysis of fine layering effects: medium averaging versus synthetic seismograms: Presented at the 59th Ann. Internat. Mtg., Soc. Expl. Geophys., Expanded Abstracts, 1083–1085.

Haskell, N. A., 1953, The dispersion of surface waves on multilayered media: Bull. Seis. Soc. Am., 43, 17–34.

Helbig, K., 1984, Anisotropy and dispersion in periodically layered media: Geophysics, 49, 364–373.

Kerner, C., 1989, Anisotropy and scattering: Presented at the 59th Ann. Internat. Mtg., Soc. Expl. Geophys., Expanded Abstracts, 1034–1038.

Krey, T., and Helbig, K., 1956, A theorem concerning anisotropy of stratified media and its significance for reflection seismics: Geophys. Prosp., 4, 294–302.

Melia, P. J., and Carlson, R. L., 1984, An experimental test of P-wave anisotropy in stratified media: Geophysics, 49, 374–378.

Payton, R. G., 1983, Elastic wave propagation in transversely isotropic media: Martinus Nijhohh Publ.

Philippe, J., and Bouchon, M., 1989, Propagation of waves with long-wavelength in thinly layered and cracked media: Presented at the 59th Ann. Internat. Mtg., Soc. Expl. Geophys., Expanded Abstracts, 1023–1024.

Postma, G. W., 1955, Wave propagation in a stratified medium: Geophysics, 20, 780–806.

Riznichenko, I. V., 1948, The propagation of seismic waves in discrete and heterogeneous media: Bull. Acad. Sci. USSR, Geographical and Geophysical Series, 13, 115–128.

Rytov, S. M., 1956, Acoustical properties of a thinly laminated medium: Soviet Phys. Acoust., 2, 67–80.